Study on a Parabolic Reflector Fed by L-band Multi-port Eleven Antenna

Jungang Yin[1] Per-Simon Kildal[2]
[1]Dept. of Electronics and Telecommunications, Norwegian University of Science and Technology,
N-7491 Trondheim, Norway.
[2]Dept. of Signals and Systems, Chalmers University of Technology, S-412 96 Gothenburg, Sweden.

Abstract: - The paper studies the properties of the far field of a primary-fed parabolic reflector fed by a four-port L-band Eleven antenna. The sum beam as well as difference beams in two orthogonal planes after the reflector, which are necessary for the mono-pulse tracking, have been numerically evaluated. In addition, the relationship between the spacing between two parallel folded dipoles and the matching as well as radiation properties has been investigated.

Key-Words: - Eleven antenna, Monopulse tracking, Aperture integration, BOR antenna

1 Introduction

Geostationary-Orbit (GSO) satellites with slight inclination angles will trace a figure 8 pattern in the sky over one day. Tracking capability is inherently demanded by the land-mobile or maritime satellite communications terminals in order to minimize the antenna pointing error to the fullest so as to avoid a degraded satellite link. Mono-pulse tracking systems were reported with very good tracking accuracy, fast dynamic response as well as comparatively low requirement on system signal-to-noise ratio, and have been utilized widespread in many of the large earth stations, ship-borne terminals and satellite-to-satellite communications [1].

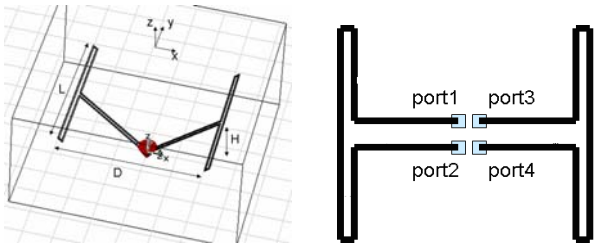

Figure 1 L-band strip model of 4-port Eleven antenna

The Eleven antenna is a new wideband feed that can so far cover a decade bandwidth up to about 13GHz, and it has been developed as feed for reflector antennas and in particular for radio telescopes [2]-[5]. Moreover, it can be further developed as a multi-port antenna that is capable of, through different combinations of excitations from these ports, producing a sum beam and two difference beams necessary for the mono-pulse tracking [6]. A parallel folded dipole pair being half-wavelength apart and above a ground plane is the basic element of the wideband Eleven antenna. The four-port L-band laboratory model is illustrated in Figure 1, and its far field properties after a reflector is of great interest to be studied for estimation of the tracking performance. Besides, the present paper also attempts to investigate how the spacing between the two parallel folded dipoles influences matching as well as radiation properties for the three different mono-pulse channels.

2 Aperture Integration (GO Reflection)

It is well known that the field equivalence principle is widely used in the analysis of aperture antennas. It replaces an aperture antenna with equivalent electric and/or magnetic currents, which produce radiation field equivalent to those from the antenna. Geometrical optics (GO) has been known as an approximate method to determine electromagnetic fields, which is asymptotically correct for high frequencies [7]. In this paper, it is reasonable for us to assume all incident fields are reflected at the parabolic surface by the classical reflection law, and then propagate along parallel straight lines, referred to as GO rays, in the free space. In addition, we also assume a circular aperture, normal to the propagation direction of GO rays, in front of the reflector. The far field after the reflector can be approximated by integration of equivalent Huygen's sources in the virtual aperture.

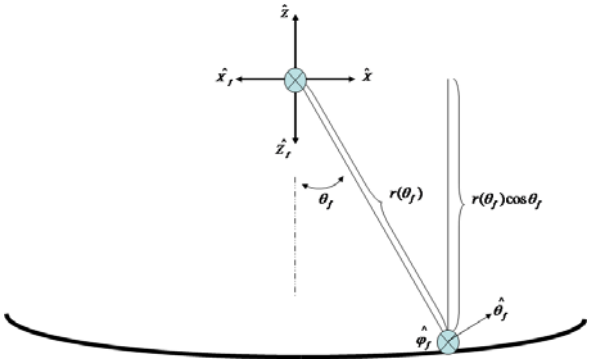

Figure 2 GO reflection at a parabolic surface

As illustrated in Figure 2, we first introduce a point source feed with its phase reference point right on the focal point of a parabolic reflector. Then we may as well create corresponding coordinate systems for the feed and for the virtual aperture in the focal plane, which is normal to $\hat{z}$ axis. Consider a general case where the feed has a far field function with arbitrary form,

$$\vec{G_f}(\vec{r}) = G_{\theta_f}(\theta_f,\varphi_f)\hat{\theta}_f + G_{\varphi_f}(\theta_f,\varphi_f)\hat{\varphi}_f \quad (1)$$

where $G_{\theta_f}(\theta_f,\varphi_f)$ and $G_{\varphi_f}(\theta_f,\varphi_f)$ are θ- and φ-components of the far field of the feed, respectively; θ_f is the polar angle and φ_f is the azimuth angle in the spherical coordinate system of the feed. As φ_f is periodic with 2π, the φ_f variation of the far field can always be expanded in a Fourier series [7],

$$\vec{G_f}(\vec{r}) = \sum_{n=0}^{\infty}\left[A_n(\theta)\sin(n\varphi_f) + B_n(\theta)\cos(n\varphi_f)\right]\hat{\theta}_f + \sum_{n=0}^{\infty}\left[C_n(\theta)\cos(n\varphi_f) - D_n(\theta)\sin(n\varphi_f)\right]\hat{\varphi}_f \quad (2)$$

Especially if the feed is y_f-polarized and symmetrical with respect to both y_fz_f-plane and x_fz_f-plane, then (2) can be reduced to [7],

$$\vec{G_f}(\vec{r}) = \sum_{n=1}^{\infty}\left[A_n(\theta)\sin(n\varphi_f)\hat{\theta}_f + C_n(\theta)\cos(n\varphi_f)\hat{\varphi}_f\right] \quad (3)$$

which indicates a sum of BOR_1(*Body Of Revolution*, n=1, i.e. the first order component of an arbitrary radiation beam when it is expressed using Fourier expansion), BOR_2 … BOR_n beams. The focal aperture field of a reflector fed by a pure BOR_1 beam has been formulated through [7: Eq.8.41-49] by assuming GO reflection. In a similar way, the focal aperture field contributed by any other order *BOR* beams can readily be analyzed as well. Thereafter, the far field of the reflector fed by them can thus be approximated by using aperture integration. For BOR_n (n>0), the focal aperture field can be expressed as follow, (4)

$$\vec{E_a}(\rho',\varphi') = -\frac{e^{-jk\cdot 2F}}{F}\cos^2(\frac{\theta_f}{2})\left[A_n(\theta_f)\sin n\varphi'\hat{\rho}' + C_n(\theta_f)\cos n\varphi'\hat{\varphi}'\right]$$
$$= -\frac{e^{-jk\cdot 2F}}{F}\cos^2(\frac{\theta_f}{2})\begin{bmatrix}(A_n(\theta_f)\sin n\varphi'\sin\varphi' + C_n(\theta_f)\cos n\varphi'\cos\varphi')\hat{y}\\ +(A_n(\theta_f)\sin n\varphi'\cos\varphi' - C_n(\theta_f)\cos n\varphi'\sin\varphi')\hat{x}\end{bmatrix}$$

where ρ' is the radial and φ' is the azimuth angle in the polar coordinate system of the focal aperture, k is the phase constant, F is the focal length, and θ_f is associated with ρ' by [7: Eq.8.32]. According to [7: Eq.6.50-51], the co-polar (y-) component of the radiation field due to the previous focal aperture field will become as,

$$\tilde{E}_{ay}(k\hat{x}\cdot\hat{r}, k\hat{y}\cdot\hat{r}) = \int_0^{d/2}\int_0^{2\pi} E_{ay}(\rho',\varphi')e^{jk\rho'\hat{\rho}'\cdot\hat{r}}d\varphi'\rho'd\rho'$$
$$= \hat{y}\frac{-e^{-jk\cdot 2F}}{F}\int_0^{d/2}\cos^2(\frac{\theta_f}{2})\rho'd\rho' \quad (5)$$
$$\cdot\int_0^{2\pi}\begin{bmatrix}A_n(\theta_f)\sin n\varphi'\sin\varphi'\\ +C_n(\theta_f)\cos n\varphi'\cos\varphi'\end{bmatrix}e^{jk\rho'\sin\theta\cos(\varphi-\varphi')}d\varphi'$$

where θ and φ are the polar and azimuth angle coordinates of the far field spherical system. Especially if θ=0, i.e. along the propagation z-axis, it can easily be found that the field in (5) turns out to be zero as long as n does not equal 1, which also applies for the cross-polar (x-) component of the far field. This implies that if an arbitrary beam is fed to a rotationally symmetric reflector, it is only its BOR_1 component that will make contribution on the propagation axis, while any of other order φ-variant components always has a null on the propagation axis. In other words, all other order φ-terms can not contribute to the on-axis gain and may thus be regarded as losses in the total radiation efficiency.

CST EMS™ is at first used to simulate the sum and difference patterns of the Eleven antenna itself. Then, both θ- and φ- components of the far field are extracted and imported into an in-house MATLAB routine for the approximation of the far field after a reflector. The primary-fed parabolic reflector in our calculation has a diameter of 2.3 meters, and the half-subtended angle is 60 degrees. According to [7: Eq.6.27], the maximum directivity from such an aperture can be achieved up to around 31.1dBi, if it is excited by a field with uniform amplitude and constant phase over the whole aperture. The difference of the actually achieved directivity and the above theoretical maximum value is usually used to evaluate the total aperture efficiency.

3 Results and Discussion

The sum channel is the communication channel for the satellite links, and the aperture efficiency as well as the return loss should be good enough to meet specific system requirements. The two difference channels take on the main task of mono-pulse tracking. The most important issues for them are, instead of the aperture efficiency or the return loss, the slope of and the cross-polar level in the co-polar null on the bore-sight axis, which could directly influence the tracking accuracy.

3.1 Sum (beam) channel

The entire far field function of a BOR_1 antenna can be constructed merely from patterns in its two principle

planes. The BOR_1 efficiency is defined as the ratio of the power in the BOR_1 component and the total radiated power, as shown below in (7), indicating how closely the far-field function resembles a BOR_1 type far-field function, as well as quantifying how much power is lost in the part of the far field that is not of BOR_1 type.

$$e_{BOR_1} = \frac{\pi \int_0^{\pi} (|G_E(\theta)|^2 + |G_H(\theta)|^2) \sin\theta d\theta}{\int_0^{2\pi}\int_0^{\pi} (|G_{CO}(\theta,\phi)|^2 + |G_{XP}(\theta,\phi)|^2) \sin\theta d\theta d\phi} \quad (7)$$

$G_{co}(\theta)$ and $G_{xp}(\theta)$ are the co-polar and cross-polar far-field functions, respectively; $G_E(\theta)$ and $G_H(\theta)$ are the first-order terms of the Fourier expansion for the θ- and φ- component of the total far-field function. If a parabolic reflector is fed by a BOR_1 beam extracted from the total far-field beam, the aperture efficiency can be factorized in a number of sub-efficiencies, including illumination efficiency, polarization efficiency, spill-over efficiency, and phase efficiency. All of the sub-efficiencies have been formulated in [7: Eq.8.62-66].

It can be seen from Figure 3 that for the total far-field beam before reflector, the cross-polar level decreases slightly as the spacing increases, since the directivity of the co-polar pattern increases slightly while the directivity of the cross-polar pattern keeps almost constant. However, for the extracted BOR_1 beam, the cross-polar level either before or after reflector will reach a peak when the spacing equals about 0.55 times wavelength, where the patterns in two principle planes greatly coincide with each other. The cross-polar level will become worse as the spacing increases further. Besides, the difference between the cross-polar level before and after reflector keeps decreasing as the spacing varies upwards.

The aperture efficiencies for both the total and extracted BOR_1 beams, as well as all sub-efficiencies, are exhibited in Figure 4. There is a clear trend indicating that the BOR_1 efficiency and the aperture efficiencies decrease as the spacing increases. The total S_{11} formulated in [6] and corresponding radiation efficiency curves for the sum channel have been plotted in Figure 5 and 6 with respect to several cases of different spacing.

3.2 Horizontal difference (beam) channel

Horizontal difference channel is expected to track the vertical-polarized beacon signal in the horizontal plane (φ=0deg). Its patterns after reflector in φ=0, 45, 90deg planes are shown in Figure 7. There is a deep dull on the bore-sight axis and the cross-polar levels are very low neighbouring the null in all φ planes. Especially, the pattern in the horizontal plane is with a very low cross-polar level. The total S_{11} and corresponding radiation efficiency curves for the horizontal difference channel with respect to different spacing are shown in Figure 8 and 9.

3.3 Vertical difference (beam) channel

Vertical difference channel is expected to track the vertical-polarized beacon signal in the vertical plane (φ=90deg), and its patterns after reflector in φ=0, 45, 90deg planes are shown in Figure 10. As we can see clearly that there is also a steep null in the centre; however, although the pattern in the vertical plane is very clean, there is a significant cross-polar level in φ=45deg plane, which implies a possible tracking ambiguity of the vertical difference channel in φ=45deg plane. Regarding this matter, we are proposing a sequential tracking procedure to overcome it. Since the horizontal difference channel has more sensitive null and lower cross-polar level, it can be used in the first place as soon as the tracking procedure starts. Ideally, it will align the target in the horizontal direction until the target reaches the neighbourhood of the vertical axis. Then the vertical difference channel can be used perform the tracking in the vertical plane, as it has a 'clean' pattern, almost free of cross-polar component. These two steps can be repeated until the tracking accuracy is achieved.

The total S_{11} and corresponding radiation efficiency curves for the vertical difference channel with respect to different spacing are shown in Figure 11 and 12. By comparison between Fig. 5, 8 and 11, we can find that when the spacing is about 0.65 times wavelength, the total S_{11} of the sum channel can be better than -10 dB over both the uplink and the downlink bands of the L-band. Meanwhile, the total S_{11} of either of the two difference channels can be no worse than -20 dB.

4 Conclusion

The far field of a primary-fed parabolic reflector fed by an L-band 4-port Eleven antenna has been numerically approximated through aperture integration assuming GO reflection. Matching and radiation properties concerning the three mono-pulse channels have been studied under different spacing between the two parallel folded dipoles. It has been shown that trade-off should be made between the aperture efficiency and the return loss (the total S_{11}), when determining the spacing. Besides, linearly-polarized beacon signal can possibly be tracked in both two orthogonal planes through a proposed

procedure. To sum up, the multi-port L-band Eleven antenna with mono-pulse tracking capability is a potential candidate to be employed in satellite communication terminals including reflectors.

References:

[1] G. J. Hawkins, D. J. Edwards, J. P. McGeehan, "Tracking systems for satellite communications", *IEE Proceedings,* **Vol. 135,** Pt. F, No.5, (1988).

[2] Per-Simon Kildal, Rikard Olsson and Jian Yang, "Development of three models of the Eleven antenna: a new decade bandwidth high performance feed for reflectors," Proceedings of EuCAP 2006, Nice, November 2006.

[3] R. Olsson, P.-S. Kildal and S. Weinreb, "The Eleven antenna: a compact low-profile decade bandwidth dual polarized feed for reflector antennas," IEEE Transactions on Antennas and Propagation, **Vol. 54**, No. 2, Pt. 1, pp.368-375, Feburary 2006.

[4] Per-Simon Kildal, "Broadband multi-dipole antenna with frequency-independent radiation characteristics", Patent application PCT/ SE2004/ 001178.

[5] Rikard Olsson, "Development of the Eleven antenna – a decade bandwidth feed for reflector antenna," Thesis for the degree of Licentiate of Engineering, Chalmers University of Technology, October 2005.

[6] J. Yin, J. A. Aas, J. Yang, P.-S. Kildal, "Monopulse tracking performance of multi-port Eleven antenna for use in satellite communications terminals", Proceedings of 2nd EuCAP, Edinburgh, UK, November 2007.

[7] Per-Simon Kildal, "Foundations of Antennas – A Unified Approach", Studentlitteratur, Sweden, 2000.

Appendix:

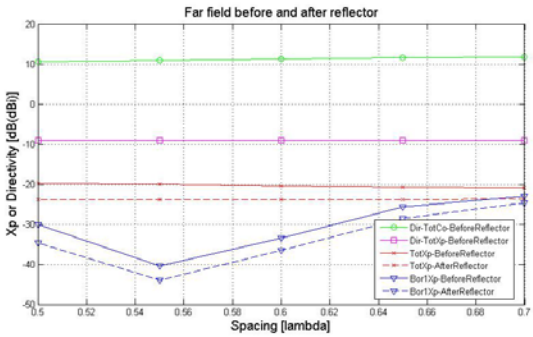

Figure 3 Directivity, Xp VS. Spacing

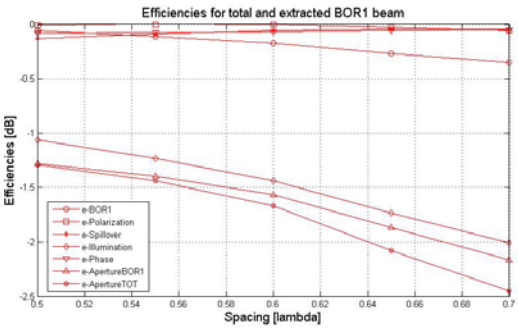

Figure 4 Aperture/sub-efficiencies VS. Spacing

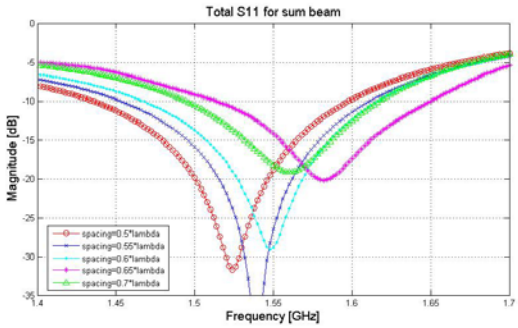

Figure 5 S_{11} VS. Spacing in sum channel

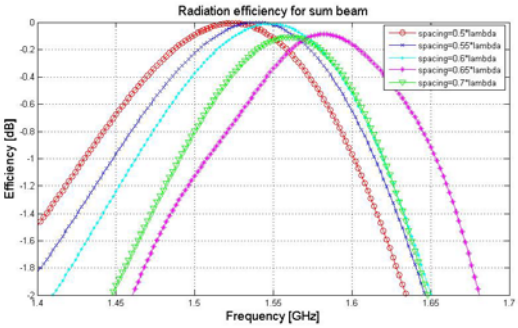

Figure 6 Radiation efficiency VS. Spacing in sum channel

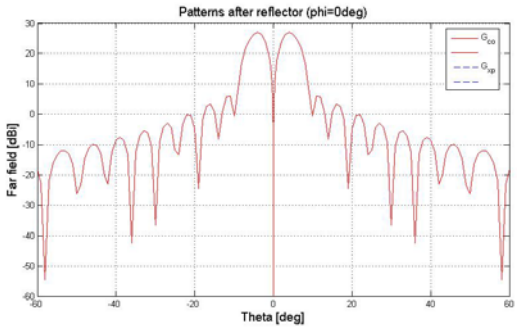

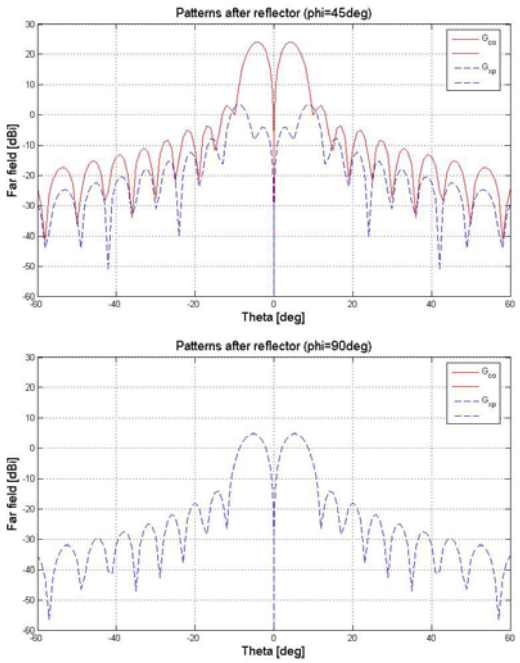

Figure 7 Horizontal difference patterns after reflector

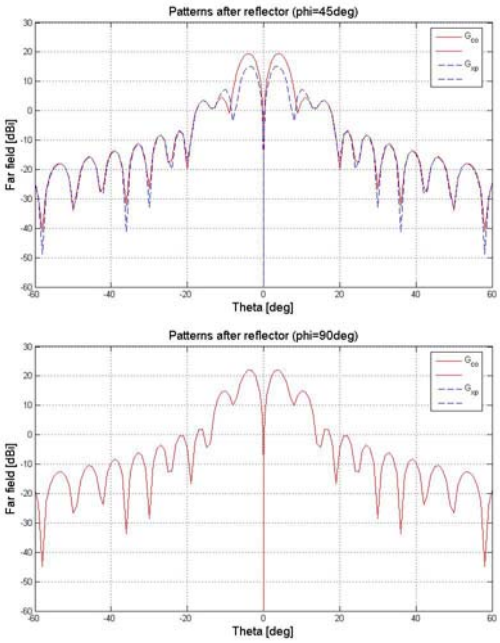

Figure 10 Vertical difference patterns after reflector

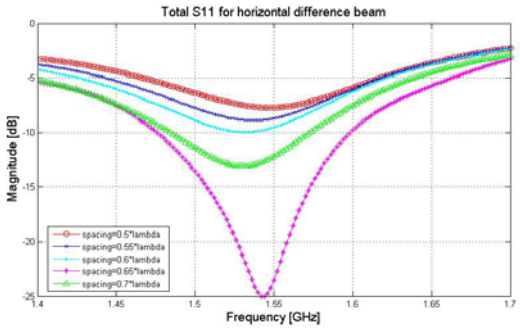

Figure 8 S_{11} VS. Spacing in horizontal difference channel

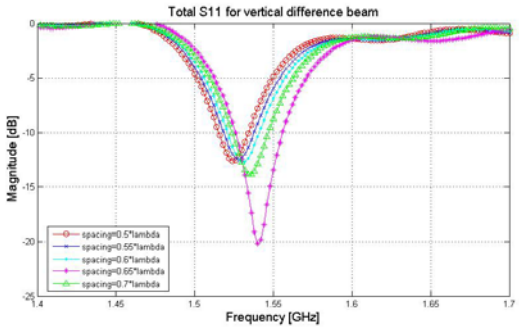

Figure 11 S_{11} VS. Spacing in vertical difference channel

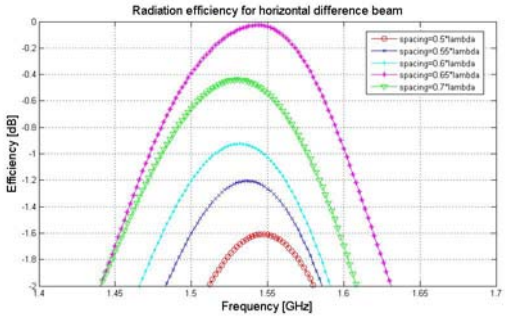

Figure 9 Radiation efficiency VS. Spacing in Δ_H channel

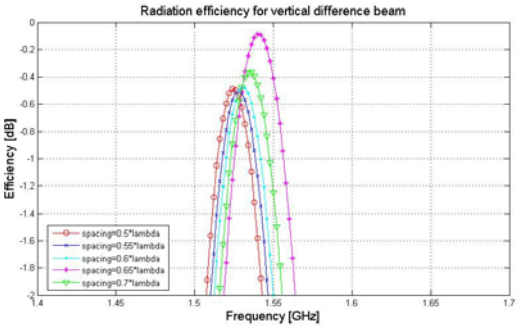

Figure 12 Radiation efficiency VS. Spacing in Δ_V channel